ISSN (Print) : 2320 – 3765
ISSN (Online): 2278 – 8875

International Journal of Advanced Research in Electrical, Electronics and Instrumentation Engineering

(An ISO 3297: 2007 Certified Organization)

Vol. 4, Issue 2, February 2015

Optimal Power Flow Analysis Considering Ramp Rate Limits of Generators

A.Pizano-Martínez[1], J.M.Lozano-García[1], E.A.Zamora-Cárdenas[1], H.J.Estrada-García[1], M.A.Gómez-Martínez[1]

Professor, Dept. of Electrical Engineering, DICIS, University of Guanajuato, Mexico [1]

ABSTRACT:This paper presents the extension of a conventional Optimal Power Flow (OPF) model to include the ramp rate limits of generators. The computational implementation of this model is carried out on the platform provided by the Matlab® optimization toolbox. The solution of the extended model allows verifying if the electric demand curve, for a given period of time, can be supplied at the minimum generation cost without violating the ramp rate limits and ratings of generators, as well as the electric network constraints. At the same time, the solution also reveals the nodal voltage profile of the whole electric network for the given electric demand curve. TheIEEE 3-machine 9-bus test system is considered to show numerical results.

KEYWORDS: Power Systems, Optimal Power Flow, Ramp Rate Limits,Matlab®.

I.INTRODUCTION

The conventional Optimal Power Flow (OPF) analysis is a very important tool to deal with economic and security aspects of electric power systems. The concept of optimal power flow, introduced by Dommel and Tinney in the early 1960's [1], has received great attention since its early application to power systems analysis [2, 3]. OPF is a nonlinear optimization problem [4], whose solution has been carried out by using a large variety of optimization techniques [2], [3], [5]. From the power system operation and control viewpoints, an OPF solution gives an answer to adjust available controls in order to meet the energy demand in the most economically manner while keeping within bounds all the constraints imposed on the system. OPF studies are being used more and more by engineers, but further applications ranging from planning, operation and control of power systems are of great interest and must be investigated [6].

The conventional OPF model has already been extended to analyze a wide range of problems associated with the operation of electric power systems. By way of example, the OPF model has been extended to; identify and analyze saddle-node and limit-induced bifurcations [7], investigate the effects of reactive power limit modeling on Maximum System Loading and Active and Reactive Power Markets [8], consider transient and voltage stability constraints [9, 10, 11] and analyze the steadystate operation of power systems with Flexible AC Transmission Systems under static security constraints [12]. Recently, the economic dispatch has received great attention to implement the tertiary control of microgrids, which is devoted to the energy management in these systems [13].

This paper presents the extension of the conventional OPF model to consider the ramp rate limits of the generators. For this purpose, the conventional model reported in [14] is adopted. Physically, the ramp rate limits represent the rate at which the output power level of given plant can be modified to satisfy the power balance [15]. The conventional OPF model ignores these constraints. In this way, the steady state operating point provided by the solution of this conventional model assumes that the output power level of any generator can be changed in the available period of time to satisfy a new power demand level. Note, however, that under that assumption, the ramp rate limits of generators could be violated. This condition would be more important if the power produced by renewable energy plants is integrated to the system.

The paper is organized as follows. The Section II provides a description of related work. The Section III of the paper shows, in general way, the mathematical extension of the conventional OPF to consider the ramp rate limit constraints. The power system components modeling and the explicit OPF formulation are presented in Section IV. The solution and the computational implementation of the extended OPF model are discussed in Section V. The prowess of the

ISSN (Print) : 2320 – 3765
ISSN (Online): 2278 – 8875

International Journal of Advanced Research in Electrical, Electronics and Instrumentation Engineering

(An ISO 3297: 2007 Certified Organization)

Vol. 4, Issue 2, February 2015

proposed implementation is illustrated by means of considering a numerical example in Section VI. The work conclusions are given in Section VII.

II.RELATED WORK

The efficient and optimum economic operation and planning of electric power systems have always occupied an important position in the electric power industry [16, 17]. The first efforts to optimize the power system operation were focused on determining the optimal generation dispatch, which encouraged the formulation and solution of the classic economic dispatch problem. The classic economic dispatch, however, is formulated as a static problem that does not "look ahead" over the future time horizon, using the predicted load trends to determine the economic allocation of generation to the load [18]. Therefore, if the power is dispatched according to the solution provided by the classic economic dispatch approach, the supply of electric power to the load may be at risk due to the ramp rate capacity of the dispatchable generators.In order to circumvent this problem, the dynamic economic dispatch problem extends the classic economic dispatch model for considering the ramp rate capacity of generators.Although the dynamic economic dispatch has been a widely studied concept [18], the topic has recently received much attention due to the development of innovative optimization techniques, the creation of competitive power markets, the integration of renewable energy resources, environmental constraints, etc.

The heuristic optimization algorithms, as differential evolution [19] and hybrid heuristic optimization [20], have been applied to solve the optimization model related to the dynamic economic dispatch problem. Also, in order to take into account the integration of renewable energy sources, the particle swarm optimization method [21] and the sequence operation theory combined with genetic algorithms [22] have been considered to solve the optimization model.Bearing in mind the operation of electric power systems within an environment of electric power markets, the dynamic economic dispatch model has been reformulated and solved in [23]. The benders decomposition method has also been considered to solve the optimization problem within the aforementioned modern power system operation context [24]. Environmental considerations were taken into account in [25], where the dynamic economic dispatch problem is solved via the particle swarm optimization method. It must be pointed out that the dynamic economic dispatch has also been enlarged to approximate the optimal energy management of microgrids [26].

The classic economic dispatch approach is close related to the OPF approach in the sense that the both optimization procedures determine the optimal power dispatch that satisfies the power demand to the lowest objective function value. Unlike the classic economic dispatch approach, however, the OPF approach can deal with transmission losses, network constraints and static security constraints, and even dynamic security constraints [27], in a very flexible way. In this sense, it is has been of interest to extend the OPF model to include the ramp rate limit of generators. The solution of this enlarged OPF model has been solved by using the evolutionary programming [28, 29], as well as hybrid particle swarm optimization and simulated annealing methods [30]. The imperialistic competitive algorithm was applied to solve a OPF model with ramp rate limits constraints and FACTS controllers embedded [31]. Similar to de dynamic economic dispatch model, the OPF model has been also enlarged to take into account ramp rate limits of generators along with environmental considerations [32], but solving the resulting problem by means of a fuzzy linear programming approach. It should be noted that the use of commercial solver packages, as AMPL, has been considered to solve the OPF model with ramp rate constraints, as reported in [33].

This work extends the conventional OPF model to consider the ramp rate limit of generators. The extended OPF is formulated as a nonlinear convex optimization problem in polar coordinates. The extension of the conventional OPF is given in the paper in detail. The resulting model can be viewed as a semi-infinite optimization problem. However, the discretization of the constraints along the time axis can also be applied to simplify the solution of the model, as described in Section V. In this way, the dynamic OPF model can be directly solved by using the “fmincon” function of the Matlab optimization toolbox [34], which simplifies the computational implementation and solution of the optimization problem.

III.GENERAL EXTENDED OPF MODEL

The ramp rate limit R constrains the rate at which the output power level of given generator can be modified from one time step $t_{z-1}$to another step t_z, where $\triangle t=t_z-t_{z-1}$. Thus, in order to satisfy a forecasted demand curve for the time interval $T=[t_0, t_1,\ldots,t_{end}]$, the ramp rate limit of each generator should be satisfied for that whole time interval T. It must be

ISSN (Print) : 2320 – 3765
ISSN (Online): 2278 – 8875

International Journal of Advanced Research in Electrical, Electronics and Instrumentation Engineering

(An ISO 3297: 2007 Certified Organization)

Vol. 4, Issue 2, February 2015

pointed out that for the purpose of simplifying the mathematical problem; the load demand curve and T were discretized at time steps t_z ($z=0,1,\ldots end$) (see Section IV). Accordingly, in order to supply the power demand at step t_z with the minimum total generation cost, a corresponding optimal operating point that satisfy the physical and operating limits of the system, as well as the ramp rate limit R constraints of the generators, at that time step must be computed. Note, however, that the generator output power levels at consecutive time steps are related by the corresponding ramp rate limit constraint. Therefore, the set of optimal operating points that satisfy the power demand for the whole set of time steps, must be computed in a unified way. According with the aforementioned discussion, the set of optimal operating points is obtained from the solution of the following extended OPF model,

$$\text{Minimize} \quad F_T = \sum_{t_z=1}^{t_{end}} f^{t_z}(\boldsymbol{y}^{t_z}) \tag{1}$$

$$\text{Subject to} \quad \boldsymbol{h}^{t_z}(\boldsymbol{y}^{t_z}) = \boldsymbol{0} \quad \forall z = 0,1,\ldots,t_{end} \tag{2}$$

$$\boldsymbol{g}^{t_z}(\boldsymbol{y}^{t_z}) \le \boldsymbol{0} \quad \forall z = 0,1,\ldots,t_{end} \tag{3}$$

$$\underline{\boldsymbol{y}} \le \boldsymbol{y}^{t_z} \le \overline{\boldsymbol{y}} \quad \forall z = 0,1,\ldots,t_{end} \tag{4}$$

$$\underline{\boldsymbol{R}} \le \Delta \boldsymbol{P}^{t_z,t_{z-1}} \le \overline{\boldsymbol{R}} \quad \forall z = 1,2,\ldots,t_{end} \tag{5}$$

where t_{end} is the last time step of the time interval T of interest. Bearing in mind that the script t_z represents the *z-esim* time step, the description of theremaining terms of (1)-(5) for each time step t_z is as follows. F_T is the objective function to be minimized, which is given as the sum of the total generation cost $f(\boldsymbol{y})$ at each time step. $\boldsymbol{h}(\boldsymbol{y})$ is a set of equality constraints representing the nodal active and reactive power balance equations. $\boldsymbol{g}(\boldsymbol{y})$ is a set of functional inequality constraints representing operating limits that depend on the system variables. $\boldsymbol{y}$ is the set of variables to be solved and it is composed by the sets of nodal voltages magnitude $\boldsymbol{V}$ and angles $\boldsymbol{\theta}$, as well as the output power of generators $\boldsymbol{P}$. The lower and upper limits of these variables are $\underline{\boldsymbol{y}}$ and $\overline{\boldsymbol{y}}$, respectively. $\underline{\boldsymbol{R}}$ and $\overline{\boldsymbol{R}}$ are the down and up ramp rate limits of generators, thus $\Delta \boldsymbol{P}$ represents the increments of $\boldsymbol{P}$ between two successive time steps t_z and t_{z-1}.

IV.EXPLICIT FORMULATION

In this section the explicit model of the power system components are firstly given. The power system components considered in this work are generators, loads, shunt compensation elements, transmission lines and transformers. Then, these explicit models are used to assemble the explicit extended OPF model in polar coordinates.

A. *Power system Modelling*

1) Generators

The generator is modeled as a controllable source of complex power, which at time step t_z provides the complex output power given by (6). Where $P_{gi}^{t_z}$ and $Q_{gi}^{t_z}$ are the active and reactive output power of the *i-esim* generator at time step t_z. The corresponding lower and upper limits are $\overline{Q}_{gi}$, $\overline{P}_{gi}$ and $\underline{P}_{gi}$, $\underline{Q}_{gi}$, respectively. If thermal units are considered, the active power production cost of the *i-esim* generator is given by (7).

$$S_{gi}^{t_z} = P_{gi}^{t_z} + jQ_{gi}^{t_z} \tag{6}$$

$$C^{t_z}(P_{gi}^{t_z}) = a_i + b_i(P_{gi}^{t_z}) + c_i(P_{gi}^{t_z})^2 \tag{7}$$

where a_i, b_i and c_i are the cost curve coefficients. The upper and lower limits of the voltage magnitude V^{t_z} of the *i-esim* generation bus are $\overline{V}_{gi}$ and $\underline{V}_{gi}$, respectively. Please, note the aforementioned upper and lower limits are not considered time dependent.An additional characteristic of the generator is its ramp rate limit R (in MW/hr). This limit represents the change in the output power level that can be achieved for a generator in a period of time $\triangle t$. This will be formulated as inequality constraint in Section III.B.

2) Loads

For the time step t_z, the power demand is considered as constant complex power consumption, stated by (8). Where $P_{li}^{t_z}$ and $Q_{li}^{t_z}$ are the active and reactive power at the *i-esim* load bus. The upper and lower bounds of the voltage magnitude V^{t_z} for the load substation are $\overline{V}_{li}^{t_z}$ and $\underline{V}_{li}^{t_z}$, respectively. These limits are not considered time dependent.

ISSN (Print) : 2320 – 3765
ISSN (Online): 2278 – 8875

International Journal of Advanced Research in Electrical, Electronics and Instrumentation Engineering

(An ISO 3297: 2007 Certified Organization)

Vol. 4, Issue 2, February 2015

$$\boldsymbol{S}_{li}^{t_z} = P_{li}^{t_z} + jQ_{li}^{t_z} \quad (8)$$

3) Shunt Compensation Element

Shunt compensation elements are described by means of a magnitude voltage dependent complex power for each time step t_z, as given by (9). The terms $P_i^{inj\,t_z}$ and $jQ_i^{inj\,t_z}$ are the active and reactive power injections provided by the *i-esim* shunt admittance connected at the bus *i*, which are explicitly described by (10) and (11), respectively.

$$\boldsymbol{S}_{sh\,i}^{t_z} = P_i^{inj\,t_z} + jQ_i^{inj\,t_z} \quad (9)$$

$$P_i^{inj\,t_z} = (V_i^{t_z})^2 G_i \quad (10)$$

$$Q_i^{inj\,t_z} = -(V_i^{t_z})_i^2 B_i \quad (11)$$

where $V_i^{t_z}$ is the voltage magnitude at the compensation node with upper and lower limits $\overline{V}_{shi}$ and $\underline{V}_{shi}$, respectively. The compensation admittance is $Y=G+jB$, where G and B are the shunt conductance and susceptance. The values of $\overline{V}_{shi}$, $\underline{V}_{shi}$, G and B are considered time independent.

4) Transmission Lines

The transmission lines are represented by the π equivalent circuit of Fig. 1, where $\boldsymbol{I}_j^{t_z}$ and $\boldsymbol{E}_j^{t_z}$ are the injected current and voltage phasors at node *i* (*i=k,m*) and time step t_z. *R*, *L* and B_c are the series resistance, series inductance and the shunt susceptance. The current-voltage relation of the equivalent circuit is given by (12)-(15).

$$\begin{bmatrix} \boldsymbol{I}_k^{t_z} \\ \boldsymbol{I}_m^{t_z} \end{bmatrix} = \begin{bmatrix} \boldsymbol{Y}_{kk} & \boldsymbol{Y}_{km} \\ \boldsymbol{Y}_{mk} & \boldsymbol{Y}_{mm} \end{bmatrix} \begin{bmatrix} \boldsymbol{E}_k^{t_z} \\ \boldsymbol{E}_m^{t_z} \end{bmatrix} \quad (12)$$

$$\boldsymbol{Y}_{kk} = \boldsymbol{Y}_{mm} = (\boldsymbol{y}_{km} + j\frac{Bc}{2}) = G_{kk} + jB_{kk} \quad (13)$$

$$\boldsymbol{Y}_{km} = \boldsymbol{Y}_{mk} = -\boldsymbol{y}_{km} = G_{km} + jB_{km} \quad (14)$$

$$G_{km} = \frac{R}{R^2 + (\omega L)^2};\ B_{km} = -\frac{\omega L}{R^2 + (\omega L)^2} \quad (15)$$

At time step t_z, the power injected at node *i* through the transmission element connected between nodes *i* and *j* , where *i=k;m, j=k,m, i≠j*, is mathematically described as follows,

$$\boldsymbol{S}_i^{t_z} = P_i^{t_z} + jQ_i^{t_z} = \boldsymbol{E}_i^{t_z} \left(\boldsymbol{I}_i^{t_z}\right)^* = \boldsymbol{E}_i^{t_z} (\boldsymbol{Y}_{ii}\boldsymbol{E}_i^{t_z} + \boldsymbol{Y}_{ij}\boldsymbol{E}_j^{t_z})^* \quad (16)$$

The Euler's identity is applied to write (16) in its real and imaginary parts,

$$P_i^{inj\,t_z} = (V_i^{t_z})^2 G_{ii} + V_i^{t_z} V_j^{t_z} \left[G_{ij} Cos(\theta_i^{t_z} - \theta_j^{t_z}) + B_{ij} Sin(\theta_i^{t_z} - \theta_j^{t_z})\right] \quad (17)$$

$$Q_i^{inj\,t_z} = -(V_i^{t_z})^2 B_{ii} + V_i^{t_z} V_j^{t_z} \left[G_{ij} Sin(\theta_i^{t_z} - \theta_j^{t_z}) - B_{ij} Cos(\theta_i^{t_z} - \theta_j^{t_z})\right] \quad (18)$$

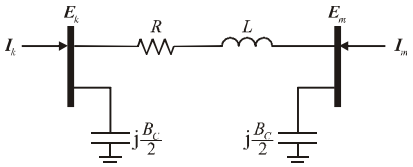

Fig. 1. Equivalent circuit of the transmission line.

Please note that in the equations of the transmission line, only the voltages and currents are time dependent.

5) Conventional Transformers

In order to simulate networks with transformers having changers at off nominal tap ratio position at either primary or secondary side, the two winding transformer is modeled with complex taps on both primary and secondary windings. The schematic equivalent circuit is shown in Fig 2.The primary winding is represented as an ideal transformer having complex tap ratios T_v:1 and T_i:1 in series with the impedance $\mathbf{Z}_p$, where $\boldsymbol{T}_v = \boldsymbol{T}_i^* = T_v \angle \phi_{tv}$ [14]. The superscript * denotes the conjugate operation. Also, the secondary winding is represented as an ideal transformer having complex tap ratios

ISSN (Print) : 2320 – 3765
ISSN (Online): 2278 – 8875

International Journal of Advanced Research in Electrical, Electronics and Instrumentation Engineering

(An ISO 3297: 2007 Certified Organization)

Vol. 4, Issue 2, February 2015

$\boldsymbol{U}_v$:1 and $\boldsymbol{U}_i$:1 in series with the impedance $\boldsymbol{Z}_s$, where $\boldsymbol{U}_v$=$\boldsymbol{U}_i$*= $U_v\angle\phi_{uv}$. The transfer admittance matrix relating the primary voltage $\boldsymbol{V}_p^{t_z}$ and current $\boldsymbol{I}_p^{t_z}$ to the secondary voltage $\boldsymbol{V}_s^{t_z}$ and current $\boldsymbol{V}_s^{t_z}$ in the two-winding transformer is,

$$\begin{bmatrix}\boldsymbol{I}_p^{t_z}\\ \boldsymbol{I}_s^{t_z}\end{bmatrix}=\left[\begin{bmatrix}G_{PP} & G_{PS}\\ G_{SP} & G_{SS}\end{bmatrix}+j\begin{bmatrix}B_{PP} & B_{PS}\\ B_{SP} & B_{SS}\end{bmatrix}\right]\begin{bmatrix}\boldsymbol{V}_p^{t_z}\\ \boldsymbol{V}_s^{t_z}\end{bmatrix} \quad (19)$$

where

$$G_{PP}=\frac{F1(U_v^2+R1)+F2R2}{F1^2+F2^2};\ B_{PP}=\frac{F1R2-F2(U_v^2+R1)}{F1^2+F2^2};\ G_{SS}=\frac{F1(T_v^2+R3)+F2R4}{F1^2+F2^2};\ B_{SS}=\frac{F1R4-F2(T_v^2+R3)}{F1^2+F2^2};$$

$$G_{PS}=-T_vU_v\left(F1\cos(\phi_1)+F2\sin(\phi_1)\right)/F1^2+F2^2;\ B_{PS}=T_vU_v\left(F2\cos(\phi_1)+F1\sin(\phi_1)\right)/F1^2+F2^2;$$

$$G_{SP}=-T_vU_v\left(F1\cos(\phi_2)+F2\sin(\phi_2)\right)/F1^2+F2^2;\quad B_{SP}=T_vU_v\left(F2\cos(\phi_2)+F1\sin(\phi_2)\right)/F1^2+F2^2;\ F1=T_v^2R_S+U_v^2R_P+\mathrm{R}_{eq1};$$

$$F2=T_v^2X_S+U_v^2X_P+X_{eq1};\ \mathrm{R}_{eq1}=(R_PR_S-X_PX_S)G_0-(R_PX_S-R_SX_P)B_0;\ X_{eq1}=(R_PR_S-X_PX_S)B_0+(R_PX_S-R_SX_P)G_0$$

$$R1=R_SG_0-X_SB_0;\ R2=R_SB_0-X_SG_0;\quad R3=R_PG_0-X_PB_0;\ R4=R_PB_0-X_PG_0;\ \phi_1=\phi_{tv}-\phi_{uv};\ \phi_2=\phi_{uv}-\phi_{tv}$$

At time step t_z, the active and reactive power injections at node i through the transformer connecting nodes i and j, where i=p,s, j=p,s, $i\neq j$, are respectively computed by using (17) and (18), but using conductances and susceptances of (19). It must be pointed out that in all the above mentioned equations of the conventional transformer, only the voltage and current phasorsvariables are time dependent.

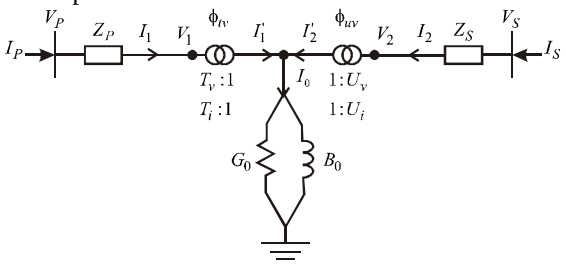

Fig. 2. Equivalent circuit of the two winding transformer

B. *OPF Explicit Model*

The OPF explicit formulation is straightforwardly assembled by considering the aforementioned models of the power system components, as given below.

6) Objective Function

The objective is to minimize (1), which is the sum of the total generation cost $f^{t_z}(\boldsymbol{y}^{t_z})$ at each time step t_z. Hence, $f^{t_z}(\boldsymbol{y}^{t_z})$ can be explicitly formulated taking into account (7), as given by (20),where a_i, b_i and c_i are the cost curve coefficients for generator connected to bus i. N_g is the number of generators, whose individual output power level is P_{gi}.

$$f^{t_z}(\boldsymbol{y}^{t_z})=\sum_{i=1}^{N_g}a_i+b_i\,(P_{gi}^{t_z})+c_i\,(P_{gi}^{t_z})^2 \quad (20)$$

7) Equality Constraints

The energy balance of the power system must be unconditionally satisfied at each time step t_z. This is enforced by means of (2), which is explicitly formulated in terms of the active and reactive power balance at each bus according to the equality constraint set (21).

$$\boldsymbol{h}^{t_z}(\boldsymbol{y}^{t_z})=\left\{\begin{matrix}P_{gi}^{t_z}-P_{li}^{t_z}-\sum_{j\in i}P_{inj\,i}^{t_z}=0,\\ Q_{gk}^{t_z}-Q_{lk}^{t_z}-\sum_{j\in k}Q_{inj\,k}^{t_z}=0\end{matrix}\right\},\ \begin{matrix}i=1,2,\ldots,N_b\\ k=1,2,\ldots,N_b|k\notin N_g\end{matrix} \quad (21)$$

where N_b is the number of buses. The active and reactive output power levels, $P_{gi}^{t_z}$ and $Q_{gk}^{t_z}$, respectively, as indicated by (5). The active $P_{li}^{t_z}$ and reactive $Q_{lk}^{t_z}$ power loads are the complex power consumption, as given by (7). $\sum_{j\in i,k}$ is the

ISSN (Print) : 2320 – 3765
ISSN (Online): 2278 – 8875

International Journal of Advanced Research in Electrical, Electronics and Instrumentation Engineering

(An ISO 3297: 2007 Certified Organization)

Vol. 4, Issue 2, February 2015

set of nodes adjacent to node *j*, whilst $P_{inj\ j}^{t_z}$ and $Q_{inj\ j}^{t_z}$ are active and reactive power flows injected at bus *j* through the network elements, according to (10), (11), (17) and (18). The reactive power balance equality constraint can be only stated for non-generation buses ($k \notin N_g$). However, the reactive power balance at generation buses is handled by means of an inequality constraint [14], as stated in the following section.

8) Inequality Constraints

The physical and operating limits of generators and substations are formulated by means of inequality constraints sets,

$$\boldsymbol{Y} = \begin{Bmatrix} \underline{P}_{gi} \le P_{gi}^{t_z} \le \bar{P}_{gi} \\ \underline{V}_j \le V_j^{t_z} \le \bar{V}_j \end{Bmatrix}, \begin{matrix} i=1,2,\ldots,N_g \\ j=1,2,\ldots,N_b \end{matrix} \quad (22)$$

$$\boldsymbol{g}(\boldsymbol{y}) = \left\{ \underline{Q}_{gi} \le Q_{gi}^{t_z} \le \bar{Q}_{gi} \right\}, i=1,2,\ldots,N_g \quad (23)$$

On the one hand, the limits of both active power generation $P_{gi}^{t_z}$ and voltage magnitude $V_j^{t_z}$ are inequality constraints on variables, such that (22) is the explicit formulation of (4). The inequality constraints (23) represent the reactive power limits of the generator and it is the explicit formulation of (3). In (23) the term $Q_{gi}^{t_z}$ is derived from (18) and (21), and is given by (24).

$$Q_{gi}^{t_z} = Q_{li}^{t_z} + \sum_{j \in i} -(V_i^{t_z})^2 B_{li} + V_i^{t_z} V_j^{t_z} \left[G_{ij} Sin(\theta_i^{t_z} - \theta_j^{t_z}) - B_{ij} Cos(\theta_i^{t_z} - \theta_j^{t_z}) \right] \quad (24)$$

The relation (24) means that the reactive power balance at the *i-esim* generation bus is always satisfied when the generator is inside its reactive power generation limits. When during the optimization process the generator hits either its lower $\underline{Q}_{gi}$ or upper $\bar{Q}_{gi}$ limit, the inequality (23) is transformed by the algorithm into the equality constraints (25) to set the reactive power generation level $Q_{gi}^{t_z}$ at the violated limit Q_{gi}^{v} ($Q_{gi}^{v} = \underline{Q}_{gi}, \bar{Q}_{gi}$). $Q_{gi}^{t_z}$ is defined by (24).

$$Q_{gi}^{v} - Q_{gi}^{t_z} = 0 \quad (25)$$

9) Ramp Rate Limits Constraints

The mathematical formulation of the ramp rate limit of the generators is given by (24), which is the explicit formulation of (5).

$$-R_i \Delta t \le P_{gi}^{t_{z-1}} - P_{gi}^{t_z} \le \Delta t R_i \quad \forall i=1,2,\ldots,N_g \quad (26)$$

where R_i is the ramp rate limit of the *i-esim* generator. Δt is the time span between any two consecutive time steps t_{z-1} and t_z. $P_{gi}^{t_{z-1}}$ and $P_{gi}^{t_z}$ are the output power levels of the i-esim generator at time steps t_{z-1} and t_z, respectively.

V. IMPLEMENTATION AND SOLUTION OF THE EXTENDED OPF MODEL

From its origin, the model required to include the ramp rate constraints of the generators is a semi-infinite programing problem. This means the optimization model has a finite number of variables, but infinite number of constraints. This is because of the amount of variables is defined by the amount nodes and generators composing the power system. Note, however, that in order to obtain a continuous solution along the time axis, the length of time step $\triangle t$ must tend to zero. In this way, the resulting number of constraints is infinite. Unfortunately, there is not optimization technique able to straightforwardly solve this kind of problem. In order to obtain an approximated solution of this problem, the time interval *T* can be discretized in a finite number of time steps t_z, which straightforwardly allows formulating a finite optimization problem. Accordingly, the resulting finite problem can be solved considering the conventional optimization theory.

The aforementioned reasoning was also used here to take into account the ramp rate limit constraints of the generators. Then, the resulting optimization model (1)-(5) is solved by using the fmincon function of the optimization toolbox of Matlab® **[**34**]**. This function is based on a Sequential Quadratic Programming optimization algorithm. In addition, the computational implementation reported in [14] was adopted and extended in this work to solve the OPF problem taking into account the ramp rate constraints of the generators. The following section shows numerical results.

ISSN (Print) : 2320 – 3765
ISSN (Online): 2278 – 8875

International Journal of Advanced Research in Electrical, Electronics and Instrumentation Engineering

(An ISO 3297: 2007 Certified Organization)

Vol. 4, Issue 2, February 2015

VI. NUMERICAL EXAMPLE

In order present numerical results, the computational algorithm developed in this work was applied to analyze the IEEE 3-machine 9-bus test system [35]. The Fig. 3 shows the schematic diagram of the system. In this diagram, the electric parameters of the network components are given in pu on a base power of 100MVA. The system voltage levels range from 13.8kV to 230kV. The generators data and ratings are given in Table I; the generator number, lower and upper active power limits, lower and upper reactive power limits, curve cost coefficients (a, b, and c) [36] and the ramp rate limits are shown from column 1 to 9, respectively. The limits of the nodal voltage magnitudes are set to $0.95 \leq V_i \leq 1.05$ pu. The total active and reactive power demand curves for a time interval T of 23 hrs are illustrated in Fig.4. It was considered that the power demand change at constant power factor. For the study, 24 time steps t_z were considered with a time step length $\triangle t$ equal to 1hr. For the purposed of this case study, both the active and reactive total power demand are shared among the three loads connected at nodes 5, 6 and 8, respectively.

The fmincon function is executed to obtain the unified solution of (1)-(5), which provides at once the set of optimal operating points that satisfy the power demand for the whole set of time steps, minimize the total generation cost, satisfy the physical and operating limits and the ramp rate limit constraints. The convergence tolerance for the fmincon function was set to $1x10^{-6}$. The columns 2 through 7 of the Table II show the resulting optimal power dispatch corresponding to the computed 24 operating points, which are illustrated in Fig. 5. Additionally, the associated nodal voltage magnitudes at nodes N_i (i=1, 2, …, 9) are illustrated in Fig. 6.a. The status of the ramp limit constraint (24) of the generators for the whole time interval T of interest is illustrated in Fig. 6.b. In this figure, a value of zero means that the constraint is not active, i.e., the generator operates below of its ramp rate limit. Values of minus one and plus one indicate that the generator is operating at either its upper or lower ramp rate limit.

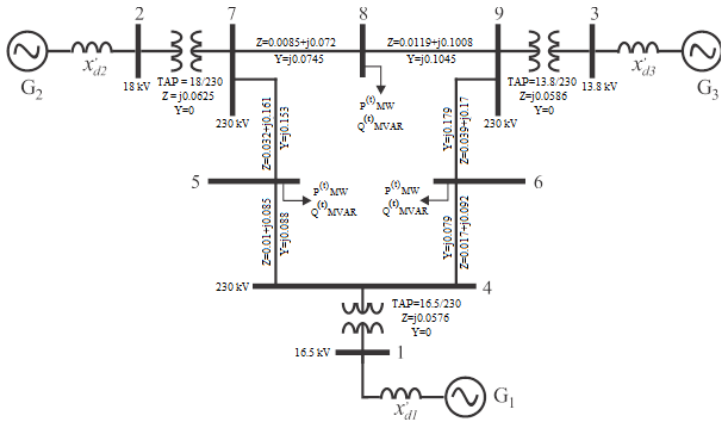

Fig. 3. IEEE 3-machine 9-bus test system.

TABLE I. GENERATORS DATA AND RATINGS

No.	P_{gimin}(MW)	P_{gimax}(MW)	Q_{gimin}(MVAR)	Q_{gimax}(MVAR)	a ($/hr)	B($/MW hr)	C($/MW^2 hr)	R(MW/hr)
G_1	0	200	-100	150	140	0.020	0.0060	15
G_2	0	150	-100	300	120	0.015	0.0075	25
G_3	0	100	-100	300	800	0.018	0.0070	30

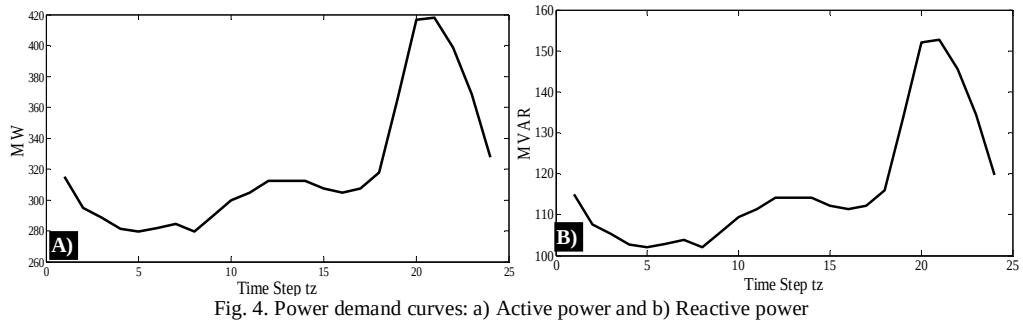

Fig. 4. Power demand curves: a) Active power and b) Reactive power

TABLE II. ACTIVE AND REACTIVE POWER DISPATCH

ISSN (Print) : 2320 – 3765
ISSN (Online): 2278 – 8875

International Journal of Advanced Research in Electrical, Electronics and Instrumentation Engineering

(An ISO 3297: 2007 Certified Organization)

Vol. 4, Issue 2, February 2015

Time step z	Active Power			Reactive Power		
	G_1	G_2	G_3	G_1	G_2	G_3
1	106.1	112.8	99.1	17.2	4.7	-15.5
2	97.7	107	92.7	12.7	0.5	-19.4
4	95.3	105.1	90.7	10.8	-0.5	-20.1
5	92.5	102.9	88.5	8.5	-1.7	-20.8
6	91.7	102.3	87.8	7.9	-2	-21
7	92.8	103	88.6	8.5	-1.5	-20.6
8	93.7	103.8	89.4	9.5	-1.2	-20.5
9	95.6	105.4	91.1	11.6	-0.6	-20.2
10	99.8	108.4	94.3	13.8	1.6	-18.6
11	101.9	109.8	95.9	14.8	2.9	-17.7
12	105.1	112.2	98.1	16.6	4.3	-16.1
13	105.1	112.2	98.1	16.6	4.3	-16.1
14	105.1	112.2	98.1	16.6	4.3	-16.1
15	102.8	110.7	96.8	15.4	3.5	-17.3
16	111.8	105	90.7	14.5	2.4	-17.8
17	126.8	98.9	84.2	15.2	1.9	-16.8
18	141.8	100	78.4	18.8	1.4	-12.7
19	156.8	125	87.7	31.1	13.6	-4.9
20	171.8	150	100	46	24.4	7
21	173.3	150	100	46.6	24.7	7.3
22	158.3	145.2	100	39.7	20.2	3.7
23	143.3	129	100	30.8	13.7	-3.3
24	128.3	108.2	94.1	20.1	6.1	-12.8

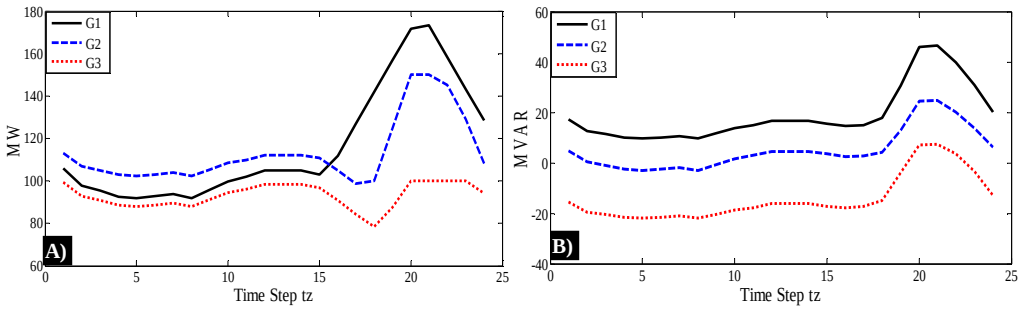

Fig. 5. Power dispatch: a) Active power and b) Reactive power

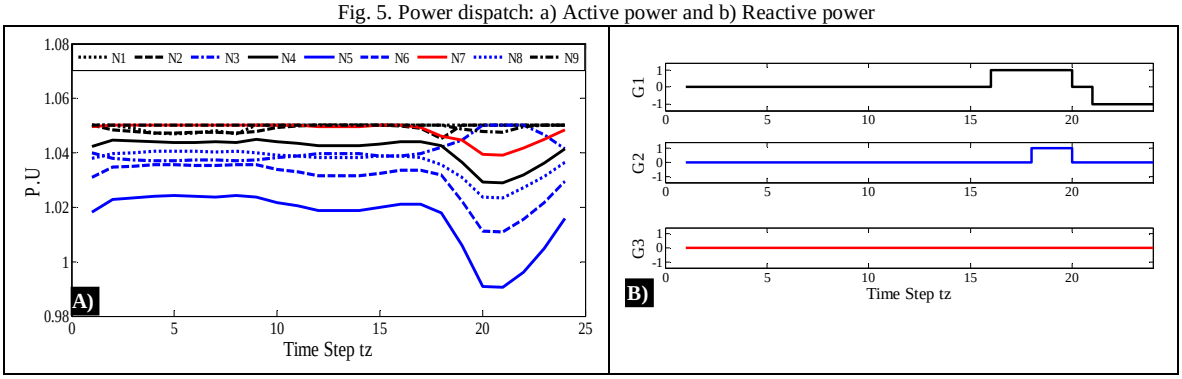

Fig. 6. Voltage profile and status of ramp limits: a) Nodal voltage magnitudes and b) Status of the ramp rate limit constraints

Based on the above results, the following remarks are stated. The results shows that the power demand curve forecasted for the time interval *T* can be satisfied by the generators; otherwise the optimization algorithm would reach an

ISSN (Print) : 2320 – 3765
ISSN (Online): 2278 – 8875

International Journal of Advanced Research in Electrical, Electronics and Instrumentation Engineering

(An ISO 3297: 2007 Certified Organization)

Vol. 4, Issue 2, February 2015

unfeasible solution. The Fig. 5 shows that the computed active and reactive power dispatch is in accordance with the active and reactive power demand curves. Note from Fig. 6.b, however, that in order to economically satisfy the power demand, the generator G1 must change its activeoutput power level from time step t_{16} to t_{20} at its upper ramp rete limit (upper limit of constraint (24) is active). This generator also changes its active output power level at its lower ramp rate limit from t_{22} to t_{24}(lower limit of constraint (24) is active). Similarly, the generator G2 operates at its ramp rate limit from time step t_{18} to t_{20}. The generator G3 does not operates at its ramp rate limit along *T*. The ramp rate limit status could be corroborated numerically from Table I by subtracting the output power of the *i-esim* generatorfor two consecutive time steps. t_z and t_{z-1}. With regard to the nodal voltages, the figure 6.a reveals that the voltages have an important decrease from t_{16} to t_{20}. This could be also expected, since the reactive power demand importantly increases during that time interval (see Fig.4.b). We highlight that based on these results, the complex power flow distribution for the entire network, and the whole interval *T*, could be readily evaluated.

VII.CONCLUSION

This work presents the extension of a conventional OPF model to consider the ramp rate limit of the generators. The extended model was solved by using the optimization toolbox of Matlab®. The unified solution of the proposed model provides a set of optimum steady state operating points that satisfy the forecasted demand curve whilst satisfying the physical and operating conditions of the power system, as well as the ramp limit constraint of the generators. The value of the whole set of network variables is known at the solution, such that the nodal voltage level can be verified for the whole interval *T*.

REFERENCES

[1] B. Stott, “Power system dynamic respond calculations”. *Proc. of the IEEE, Special Issue on Computers in Power System Operations*, Vol. 67, No. 2, pp. 219-241, Feb. 1979.
[2] M. Huneault and F. D. Galiana, "A survey of the optimal power flow literature". *IEEE Trans. on Power Syst.*, Vol.6, No.2, pp.762-770, May 1991.
[3] J.A. Momoh, "Optimal Power Flow with Multiple Objective Functions". *Proc. of the 1989 IEEE North American Power Symposium*, pp.105-108.
[4] J. A. Momoh, M.E. El-Hawari, and R. Adapa, “A review of selected optimal power flow literature to 1993: part I: nonlinear and quadratic programming approaches”. *IEEE Trans. Power Syst.*, Vol. 14, No. 1, pp. 96-104, February 1999.
[5] J. A. Momoh, M.E. El-Hawari, and R. Adapa, “A review of selected optimal power flow literature to 1993 part II: Newton, linear programming and interior point methods”. *IEEE Trans. Power Syst.*, Vol. 14, No. 1, pp. 105-111, February 1999.
[6] J.A. Momoh, R.J. Koessler, M.S. Bond, B. Stott, and D. Sun, A. Papalexopoulos and P. Ristanovic, “Challenges to optimal power flow”. *IEEE Trans. Power Syst.* Vol. 12, No. 1, pp. 444-455, Feb. 1997.
[7] R. J. Avalos, C.A. Cañizares, F. Milano, and A. J. Conejo, “Equivalency of Continuation and Optimization Methods to Determine Saddle-Node and Limit-Induced Bifurcations in Power Systems”. *IEEE Trans. on Circuits and Systems*, Vol. 56, No. 1, pp. 210-223, January 2009.
[8] B. Tamimi, C.A. Cañizares, and S. Vaez-Zadeh, “Effect of Reactive Power Limit Modeling on Maximum System Loading and Active and Reactive Power Markets” *IEEE Trans. on Circuits and Systems*, Vol. 25, No. 2, pp. 1106-1116, May 2010.
[9] V.J. Gutierrez-Martinez, C.A. Cañizares, C.R. Fuerte-Esquivel, A. Pizano-Martínez, and X. Gu, “Neural-network security-boundary constrained optimal power flow”. *IEEE Trans. Power Syst.*, Vol. 26, No.1, pp.63-72, Feb., 2011.
[10] Pizano-Martínez A., Fuerte-Esquivel C.R., and Ruiz-Vega D., “Global Transient Stability-Constrained Optimal Power Flow using SIME Sensitivity analysis,” *IEEE-PES General Meeting 2010*, pp. 8, July 2010.
[11] R. Zárate-Miñano, T. Van Cutsem, F. Milano and A. J. Conejo, “Securing transient stability using time-domain simulations within an optimal power flow”. *IEEE Trans. on Power Syst.*,Vol.25, No.1, pp. 243-253, Feb. 2010.
[12] I. Catherine Divya and Dr. S. Nagalakshmi, “Comparison of Mincut and Differential EvolutionAlgorithms for SCOPF with FACTS Devicesunder normal and n-1 contingency conditions,” IJAREEIE, Vol.3, No. 4. pp.9159-9167, April 2014.
[13] Bidram, A.; Davoudi, A., "Hierarchical Structure of Microgrids Control System,"*IEEE Trans. onSmart Grid*, Vol.3, No.4, pp.1963-1976, 2012.
[14] Pizano-Martínez, A., Fuerte-Esquivel, C., Zamora-Cárdenas, E.A., and Segundo Ramírez, J., “Conventional Optimal Power Flow Analysis Using the Matlab Optimization Toolbox,” IEEE ROPEC International 2010, pp. 6, Nov. 2010.
[15] K. Asano and T. Kumano,"Dynamic economic load dispatch by calculus of variation considering ramp rate," *Proc. of the 2007 Power Engineering Conference, IPEC 2007*, pp.167-172, 2007.
[16] A. J. Wood and B. F. Wollenberg, Power Generation, Operation, and Control. 2nd ed., John Wiley and Sons, 1984.
[17] Mohd Javed Khan and Hemant Mahala, “Particle Swarm Optimization by NaturalExponent Inertia Weight for Economic loadDispatch,” IJAREEIE, Vol.3, No. 12. pp.13657-13662, April 2014.
[18] D. W. Ross and Sungkook Kim, “Dynamic Economic Dispatch of Generation”. IEEE Trans. on Power Apparatus and Systems, Vol.PAS-99, No.6, pp.2060-2068, Nov./Dec.1980.
[19] N. Noman and H. Iba, "Solving dynamic economic dispatch problems using cellular differential evolution,"IEEE Congress on Evolutionary Computation (CEC) 2011, pp. 8, June 2011.
[20] W. Ongsakul and Ruangpayoongsak, N., "Constrained dynamic economic dispatch by simulated annealing/genetic algorithms," *Proc. of the 2001 Power Industry Computer Applications*, pp.207-212, 2001.

ISSN (Print) : 2320 – 3765
ISSN (Online): 2278 – 8875

International Journal of Advanced Research in Electrical, Electronics and Instrumentation Engineering

(An ISO 3297: 2007 Certified Organization)

Vol. 4, Issue 2, February 2015

[21] F.S. Abu-Mouti and M.E. El-Hawary,"Optimal dynamic economic dispatch including renewable energy source using artificial bee colony algorithm," *Proc. of the 2010 Systems Conference*, pp.1-6, 2010.
[22] Dewei Liu, Jianbo Guo, Yuehui Huang, Weisheng Wang, and Ping Wang, "A dynamic economic dispatch method of wind integrated power system considering the total probability of wind power," IET Renewable Power Generation Conference (RPG 2013), pp.4, Sept. 2013.
[23] Y. Chien-Ning, A. I. Cohen and B. Danai,"Multi-interval optimization for real-time power system scheduling in the Ontario electricity market," IEEE Power Engineering Society General Meeting 2005, pp.2717-2723, June 2005.
[24] J. Martínez-Crespo, J. Usaola and J.L. Fernández, "Optimal security-constrained power scheduling by Benders decomposition", Electric Power Systems Research, Vol. 77, No. 7, pp 739-753, May 2007.
[25] Y. Guan, Y. Wang and Z. Tan, "Environmental Protection and Security Considered Dynamic Economic Dispatch for Wind Farm Integrated Systems," IEEE Asia-Pacific Power and Energy Engineering Conference (APPEEC) 2012, pp. 4, March 2012.
[26] L. Xiaoping, D. Ming, h. Jianghong, H. Pingping, y P. Yali,"Dynamic economic dispatch for microgrids including battery energy storage," *Proc. of the 2010 Power Electronics for Distributed Generation Systems (PEDG)*, pp.914-917, 2010.
[27] A. Pizano-Martínez, C.R. Fuerte-Esquivel, A. Zamora-Cárdenas, and D. Ruiz-Vega," Selective Transient Stability-Constrained Optimal Power Flow Using a SIME and Trajectory Sensitivity Unified Analysis", Electric Power Systems Research, Elsevier, ISSN 0378-7796, Vol. 109, No. 3, pp.32-44, April 2014.
[28] R. Gnanadass, P. Venkatesh and N. Prasad Padhy,"Evolutionary Programming Based Optimal Power Flow for Units with Non-Smooth Fuel Cost Functions," Electric Power Components and Systems, Vol.33, No. 3, pp. 349-361, 2004.
[29] B. Mahdad and K. Srairi, "A Study on Multi-objective Optimal Power Flow under Contingency using Differential Evolution," J. Electr. Eng. Technol. (JEET) Vol. 8, No. 1, pp.53-63, 2013.
[30] T. Niknam, M.R. Narimani and M. Jabbari, "Dynamic optimal power flow using hybrid particle swarm optimization and simulated annealing," International Transactions on Electrical Energy Systems, Vol. 23: No. 7, pp. 975–1001, October 2013.
[31] G. Nageswara Reddy, S. S. Dash, S. Sivangaraju and Ch. V. Suresh, "Optimal Power Flow in the Presence of Practical Constraints and with TCSC using Imperialistic Competitive Algorithm," Global Journal of Researches in Engineering, Vol. 14, No. 8, pp. 14-22, 2014.
[32] K. Chayakulkheeree,"Unified multi-objective optimal power flow considering emissions with fuzzy network and generators ramp-rate constraints," Electrical Engineering/Electronics, Computer, Telecommunications and Information Technology (ECTI-CON) 2011, pp.832-835, May 2011.
[33] W. A. Bukhsh,C. Zhang, P. Pinson, "A Multiperiod OPF Model Under Renewable Generation Uncertainty and Demand Side Flexibility," Cornell University Library: math.OC,pp. 8, 2014.
[34] The MathWorks, Inc., "Matlab Optimization Toolbox," Users Guide Version 2, available athttp://www.mathworks.com.
[35] P. W. Sauer and M. A. Pai. *Power System Dynamics and Stability*. Prentice-Hall, 1998.
[36] T. B. Nguyen and M. A. Pai, "Dynamic security-constrained rescheduling of power systems using trajectory sensitivities," IEEE Trans. Power Syst., Vol. 18, No. 2, p.p. 848–854, May 2003.

BIOGRAPHY

Alejandro Pizano-Martínez received his Ph.D. degree from de San Nicolás de Hidalgo, Mexico in 2010. Currently he is Professor at the Electrical Engineering Department, DICIS, University of Guanajuato, Mexico.

José M. Lozano-García received his Ph.D. degree from Cinvestav Gdl., Mexico in 2011. Currently he is Professor at the Electrical Engineering Department, DICIS, University of Guanajuato, Mexico.

Enrique Arnoldo Zamora Cárdenas received his Ph.D. degree from Universidad Michoacana de San Nicolás de Hidalgo, Mexico in 2010. Currently he is Professor at the Electrical Engineering Department, DICIS, University of Guanajuato, Mexico.

Héctor J. Estrada-Garcíareceived his Ph.D. degree from CICESE, Mexico in 2008. Currently he is Electrical Engineering Department Head at DICIS, University of Guanajuato, Mexico**.**

Miguel A. Ángel Gómez Martínez. received his Ph.D. degree from Universidad Michoacana de San Nicolás de Hidalgo, Mexico in 2006. Currently he is Professor at the Electrical Engineering Department, DICIS, University of Guanajuato, Mexico.